Chemical Composition and Mass Size Distribution of PM_1 at an Elevated Site in Central East China

Y.M. Zhang[1], X.Y. Zhang[1,*], J.Y. Sun[1], G.Y. Hu[2], X.J. Shen[1], Y.Q. Wang[1], T.T. Wang[3], D.Z. Wang[4], Y. Zhao[4]

1. Key Laboratory of Atmospheric Chemistry, Chinese Academy of Meteorological Sciences, Beijing, China;
2. School of Electronic Information, Wu Han University, Wuhan, China
3. Heilongjiang Province Meteorological Bureau, Harbin, China
4. Tai An meteorological bureau, Shan Dong province, Tai' an, China

* Correspondence to X.Y. Zhang (xiaoye@cams.cma.gov.cn)

Abstract. Size-resolved aerosol chemical compositions were measured continuously for one and half years from June 2010 to January 2012 with an aerosol mass spectrometer (AMS) to characterize the mass and size distributions (MSDs) of major chemical components in submicron particles (approximately PM_1) at Mountain Tai, an elevated site in Central East China (CEC). The annual mean mass concentrations of organic, sulfate, nitrate, ammonium and chloride were 11.2, 9.2, 7.2, 5.8 and 0.95 μg m^{-3}, respectively, which are much higher than those at most mountain sites in the USA and Europe, but lower than those at the nearby surface rural sites in China. A clear seasonality was observed for all major components throughout the campaign with low concentration in fall and high in summer, and is believed to be caused by seasonal variations in planetary boundary layer (PBL) height, near surface pollutant concentrations and regional transport processes. Air masses were classified into categories impacted by PBL, lower free troposphere (LFT), new particle formation (NPF), in-cloud processes and polluted aerosols. Organics dominated the PM_1 mass during the NPF episodes, while sulfate contributed most to PM_1 in cloud events. The average MSDs of particles between 30–1000 nm during the entire campaign for organics, sulfate, nitrate, and ammonium were approximately log-normal with mass median diameters (MMDs) of 539, 585, 542, and 545 nm, respectively. These values are slightly larger than those observed at ground sites within the North China Plain (NCP), likely due to the relative aged and well-mixed aerosol masses at Mt. Tai. There were no obvious differences in MMDs during the PBL, LFT, in cloud and polluted episodes, but smaller MMDs, especially for organics, were observed during the NPF events. During the PBL, NPF and polluted episodes, organics accounted for major proportions at smaller modes, and reached to 70% at 100-200nm particles in the polluted events. In cloud episodes, inorganics contributed 70% to the whole size range dominated by sulfate, which contributed 40% to small particles (100-200nm), while organics occupied 20%, indicating that sulfate is critical chemical component in cloud formation. Seven clusters of air masses were classified based on 72-hour back trajectory analysis. The majority of the regionally-dispersed aerosols were found to be contributed from short distance mixed aerosols, mostly originated from the south with organics and sulfate as major components. Air masses from long range transport always brought clean and dry aerosols which resulted in low concentrations at the Mt .Tai. AMS-PMF (Positive Matrix Function) was employed to resolve the subtype of organics. Oxygenic organics aerosols occupied 49%, 56%, 51% and 41% of OA in the four seasons respectively, demonstrating that most OA were oxidized in summer due to strong photochemical reactions. Biomass burning organics aerosols (BBOA) accounted for 34% of OA in summer mainly from field burning of agriculture residues, and coal combustion organics aerosols (CCOA) accounted for 22% of OA in winter from heating.

Key words: Chemical Composition, Mass-size distribution, PM_1, Central East China

1 Introduction

Atmospheric aerosol particles, especially the fine particles that have relatively long atmospheric residence times, not only damage human health (Ramgolam et al., 2009), but also: (1) affect the earth's radiative balance by scattering and absorbing solar radiation, (2)indirectly influence the earth's radiative balance, cloud albedo and precipitation by serving as nuclei for cloud droplets. (Charlson et al., 1992;Solomon et al., 2007;Twomey, 1974;Albrecht, 1989). Despite of the growing recognition of their importance for human health and earth systems, the uncertainties of magnitudes of these effects are still large (Solomon et al., 2007). In fact, the influence of regionally dispersed fine aerosols on weather-climate becomes more important than that immediately influenced by local specific source and by coarser particles, whose chemical composition and size distribution are two critical parameters. The size distributions of the principal fine particle constituents also have important impacts on visibility (Watson, 2002), aerosol radiative properties and aerosol-nucleating ability (Boucher et al., 2013). The mass-size distributions (MSDs) of chemical components of fresh and aged aerosol are also critical for improving the simulation and validation of the aerosol size distributions and their optical properties (Zhou et al., 2012). Differing from conditions at ground level, the atmosphere in mountainous areas tends to have lower temperature, higher relative humidity (RH) and more intense solar radiation (Decesari et al., 2005;Li et al., 2011;Seinfeld et al., 2004). Tropospheric aerosols over mountains are most often derived from long-range transport, and therefore samples from high elevations are often representative of regional- to large-scale atmospheric conditions (Li et al., 2011;Wang et al., 2011).

As to the global scale, tropospheric aerosols are highly variable in time and space, in which the aerosol chemical components over China are found to be much higher than those in majority areas of the world, except for urban area in South Asia (Zhou et al., 2012). The sampling site in this study, Mountain Tai (Mt. Tai), is located in the Central East China with a peak elevation of ~1500 m (a.s.l). As the tropospheric aerosols over mountains are most often representative of regional- to large-scale mixed origins (Li et al., 2011;Wang et al., 2011), Mt Tai is optimal for investigating the regionally dispersed pollution. The second feature of Mt. Tai is the high frequency with which clouds envelop at the mountain peaks and provides a region where the interaction of aerosols with clouds can be studied over extended periods of time. Although there are some recent studies that investigated particulate concentrations at Mt. Tai, they have been limited on the measurement of organic molecular compositions (Fu et al., 2008), gas-phase total peroxides (Ren et al., 2009), role of biogenic volatile organic compounds (Fu et al., 2010), the impact of open crop residual burning on O_3, CO, black carbon (BC or called EC) and organic carbon (OC) (Yamaji et al., 2010), EC-OC and inorganic ions in PM_{10} during spring time (Wang et al., 2011), individual particle analysis (Li et al., 2011). These works were only limited on one or two seasons with daily sampling resolutions. No systematic measurements with high time resolution of chemical components MSDs in fine aerosol particles, covered four seasons were reported yet. It is essential to accurately and objectively assess the characterization of various chemical components and their size distribution of fine aerosols in high atmospheric level in CEC.

This paper presents a data set covering one and half years of measurement of the mass concentrations and size distributions of selected chemical components in PM_1. The purpose is to assess the regionally representative concentration levels of different aerosol chemical components, and to obtain the seasonal variations. In terms of the high altitude of the site prone to be influenced by PBL, LFT, cloud events, through the identification of relative fresh (associated with new particle formation event) and polluted aerosol, and aerosols in planet boundary layer (PBL), lower free troposphere (LFT) and in cloud, the MSDs of organic, sulfate, nitrate and ammonium under different conditions were estimated for better characterizing the aerosol chemical compositions of well-mixed aerosol and also for model verification. As the site is often influenced by regional-scale transported pollutants, the chemical and size properties of PM_1 from different air masses are also discussed. Finally, the secondary organic aerosol (SOA) fraction and primary organics aerosol

(POA) are subtyped by using a positive matrix factorization method (PMF), the mass loading level and contribution of different types of organics are presented and discussed.

2 Experimental

2.1 Campaign description

As part of the aerosol-cloud interaction campaign, supported by National Key Project of Basic Research, the aerosol chemical composition analyses were conducted at the summit of Mt. Tai (36.251°N, 117.101°E), located in Shandong Province of China with the highest elevation (1534 m a.s.l) in CEC and settled along the pathway of Asian continental outflow. Tai'an is the nearest small city, 15 km away in the south with ~500 000 population while Jinan, the capital city of Shandong Province (population: 2.1 million) is 60 km away in the north. Because the elevation of Mt. Tai station is close to the top of the planetary boundary layer, and the sampled aerosols are representative of the region rather than the immediate locality, it is a suitable site for investigating the regionally dispersed aerosol pollution over the heavily polluted CEC.

From June 2010 to January 2012, an aerosol mass spectrometer (Q-AMS, Aerodyne Research Inc. Boston, MA, USA) was used to measure the mass concentrations (30 nm-1 μm) of organics, sulfate, nitrate, ammonium and chloride in MS-mode with 5 minutes time resolution (Jayne et al., 2000;Zhang et al., 2011). The sampling periods for the AMS study were from 24 June-15 August, 22 September-11 October in 2010, 26 March-20 April, 5 June-30 June, 22 October-1 December in 2011 and 22 December 2011-13 January 2012. As a result of interruptions due to calibration, instrument failures and local burning events, 123 days of valid data were obtained. From July to December in 2010, a scanning mobility particle sizer (SMPS) (TSI 3936, TSI Inc.) was also used to monitor the number size distribution of aerosols over a size range of 10-680 nm at a time resolution of 5 minutes (2.5 minutes per scan, two scans) (Zhang et al., 2011). From December 25, 2010 until the end of the study, a tandem differential mobility particle sizer (TDMPS, IFT, Leibniz Institute for Tropospheric Research, Germany) and an aerodynamic particle sizer (APS, model 3321, TSI Inc., St Paul, USA) were used instead of the SMPS for particle number size distribution (PNSD) measurements. Together these two instruments covered particles from 3 nm to 2.5 μm in diameter. To correct the concentrations for bounce at the vaporizer and the partial transmission of particles by the lens, a fixed particle-collection efficiency factor of 0.5 was used, which was obtained in studies conducted in Beijing (Sun et al., 2010;Zhang et al., 2011;Zhang et al., 2012d), and a comparison of results presented below indicates that a reasonable correction was conducted.

Detection limits (DLs) for the AMS mass concentration were evaluated based on the mass spectra of particle-free ambient air, that is, air filtered with a HEPA filter. The DLs were defined as three times the standard deviation of each species signal in the particle-free air. During this study, the DLs for sulfate, nitrate, ammonium, organics and chloride for the 5 min averaged data were 0.03, 0.017, 0.063, 0.101, and 0.01 μg m^{-3}, respectively (Zhang et al., 2011).

The room temperature was controlled at 25 ± 3 °C, 40–60% for relative humidity (RH) and atmospheric air was sampled through a PM_{10} impactor, which was followed by a $PM_{2.5}$ cyclone (the flow rate was 16.7 L min^{-1}) and dried to a RH <30% with the use of an automatic aerosol dryer unit (Tuch et al., 2009).

2.2 Quality Assurance of the Data

To validate the assumed collection efficiency and demonstrate the data quality of our measurements, a plot of the NR-PM_1 mass concentration from the AMS against the reconstructed mass obtained with the SMPS/TDMPS is shown in Figure 1. Here, the SMPS/TDMPS dry mass concentrations were obtained by converting the measured SMPS/TDMPS number distributions to volume distributions which were then integrated into total volume, multiplied with the aerosol density and then SMPS/TDMPS mass was calculated. The aerosol density used in SMPS/TDMPS mass

calculations was assumed to be that of the average composition of $(NH_4)_2SO_4$, NH_4NO_3 and organics, whose densities are 1.77, 1.72, and 1.3 g cm^{-3}, respectively. As noted above, fixed collection efficiency (CE) of 0.5 was assumed for the entire campaign, which generally yielded a good correlation between the AMS and reconstructed SMPS/TDMPS mass data. The coefficient of determination (r^2) of AMS mass versus SMPS/TDMPS mass was 0.744 with a slope of 0.984, demonstrating a good level of agreement in the masses obtained by the two methods.

2.3 Data Separation of PBL, LFT , NPF, in cloud, polluted and Different Air-masses

Characterization of air masses sampled at the site from either PBL or LFT is important to the subsequent analysis of the chemical data. In this study, the criteria developed by (Gallagher et al., 2011) were used to differentiate the data influenced by the PBL versus the LFT. Data during night time (00:00-06:00) were considered to have been influenced by the LFT. The day time between 8:00 and 20:00 with enhanced water vapour and high aerosol concentration at the mountain top was considered to be a signal of PBL influence on the mountain. The NPF events were identified based on the evolution of the size distributions and particle number concentrations following Kulmala's definitions (Kulmala et al., 2004). The in-cloud events were picked up based on the meteorological data when the relative humidity is in range of 95%-100% with no rain event. The polluted episodes were the periods with high mass concentration and high number concentration for accumulation mode particles.

To characterize the long range transport pathways, 72-h back trajectories were computed every 6 h (00:00,6:00,12:00 and 18:00 UTC) using the HYSPLIT-4.8 (Hybrid Single Partical Lagrangian Integrated Trajectories) model of the National Oceanic and Atmospheric Administration, USA (NOAA) (http://www.arl.noaa.gov/ready/hysplit4. html). The resolution of the terrain data in the HYSPLIT model is 1º×1º, thus the real height of the mountain site has been smoothed. Therefore, 1500 m above the model ground level was chosen as trajectory start height, which is about 840 hPa in the model and is a little lower than the pressure of the measurement site (845 hPa). TrajStat (Wang et al., 2009), a program using trajectory statistical analysis data to identify potential source pathways and locations from long-term air pollution measurements, was used to construct clusters from the air-mass trajectories for long range transport pathways study. The Global Data Assimilation System (GDAS) meteorological data archives of the Air Resource Laboratory, NOAA, were used as the input.

3 Results and Discussions

3.1 Mass concentration of chemical components

The annual mean mass concentrations of organics, sulfate, nitrate, ammonium and chloride (OSNAC) in PM_1 were 11.2, 9.2, 7.2, 5.8 and 0.95 μg m^{-3}, respectively, totalling ~34.3 μg m^{-3}. This PM_1 concentration is roughly half of the ground-based values at urban Beijing (~ 500 km northwest of the Mt. Tai) (~76 μg m^{-3}) (Zhang et al., 2012d), lower than that in sub-urban Gucheng station (~52 μg m^{-3}), ~38% of the sub-urban Tianjin level (~ 80 km southeast from Beijing), and lower than those at several urban/rural sites in the Pearl River Delta in China (Xiao et al., 2011). It is higher than those in several European cities (10-30 μg m^{-3}) (Lanz et al., 2007) and some field campaigns conducted at various ground sites in urban areas, downwind of urban areas, and rural/remote locations in the mid-latitudes of the Northern Hemisphere (Zhang et al., 2007), comparable to that of Mexico City (Volkamer et al., 2006). The mass concentrations of chemical components in PM_1 at Mt. Tai are about factor of 2-3 lower (for organics and sulfate), and slightly lower (for nitrate, ammonium and chloride) than those at the near surface rural areas of China (Zhou et al., 2012). The mass loading of Mt. Tai is much higher than those at other elevated sites such as Whistler Mountain (Sun et al., 2009) , Mt. Jungfraujoch (Cozic et al.,2008), Himalayan station in Nepal (Decesari et al., 2010). The chemical components of PM_1 in spring for this study

are about 45% of the previous research results during March-April in 2009 from filter results in PM_{10} (Wang et al., 2011), which was carried out at the same site. But they are larger than those high altitude sites in Europe, Japan, India and USA in TSP, PM_{10} or $PM_{2.5}$ (Table 1).

Seasonally, the average concentrations of PM_1 in spring, summer, fall and winter were 30 μg m^{-3}, 55 μg m^{-3}, 18 μg m^{-3} and 37 μg m^{-3} respectively, which is similar with previous research for $PM_{2.5}$ (Zhou et al., 2009) at Mt. Tai (Table 1), but shows somewhat difference from typical seasonal patterns of winter minimum and summer maximum at Mt. Jungfraujioch (Cozic et al., 2008). For Mt. Tai, in summertime, plenty of VOCs, gas phase pollutants, active photochemistry, and stagnant meteorological conditions on regional scale resulted in the high concentration of chemical species within the boundary layer. With enhanced thermally driven convection, the vertical transport of ground pollutants influences the site largely. The minimum concentrations in fall would be related to the weak vertical mixing, reduced emission from ground and the active horizontal regional transport from clean places. In winter, although the site was more easily influenced by LFT for weak vertical transport, the pollutants from coal combustion for heating would increase the mass concentration of near surface aerosols and causing relative high concentration at the Mt. Tai through vertical convection.

Table1. The concentration of main aerosol chemical species at Mt. Tai compared to other Mountain stations. Data are provides in μg m^{-3}.

Location	Height (m)	Period	Size range	Organics	OC	EC	SOC	Sulfate	Nitrate	Ammonium	Reference
Mt. Tai, China	1534	Annual (2011)	PM_1	11.2				9.2	7.2	5.8	This study
		Spring (2011)		8.6				7.3	8.8	5.6	
		Summer (2010, 2011)		16.4				20.1	8.3	11.0	
		Fall (2010, 2011)		5.7				5.7	3.8	2.9	
		Winter (2011)		11.6				8.7	9.6	6.8	
		March-April 2009	PM_{10}		13.0	3.3	7.9	16.0	20.0	12.0	(Wang et al., 2011)
		From southly			12.0	2.7		21.0	23.0	16.0	
		From Northly			13.0	2.8		14.0	18.0	10.0	
		Sprig 2007	$PM_{2.5}$					12.8	5.8	5.6	(Zhou et al., 2009)
		Summer 2007						22.9	4.0	8.0	
Mt. Hua, China	2060	March-April 2009	PM_{10}		5.9	1.4	2.1	13.0	5.0	2.5	(Wang et al., 2011)
Mt. Waliguan, China	3816	Oct-1994	TSP					0.2	0.2	0.3	(Yang et al., 1996)
Zhuzhang, China	3583	Jul.2004–Mar.2005	PM_{10}		3.1			1.6	0.5	0.2	(Zhou et al., 2012)
Mt. Yulong, China	3100	Jan-Feb 2010	TSP					1.8	0.6	0.4	(Zhang et al., 2012b)
Lhasa, China	3363	Annual 2006	PM_{10}		21.0	3.7					(Zhang et al., 2008)
Mt. Whistler, Canada	2182	Spring 2006	PM_1	1.1				0.6		0.2	(Sun et al., 2009)
Mt. Jungfraujoch, Switzerland	3580	July-August 2005	TSP	1.7				0.1	0.1	0.04	(Henning et al., 2003)
		July-August 2005	PM_1	1.3				0.6	0.1	0.3	(Cozic et al., 2008)
NCO-P, Nepal	5079	Apr 2006-May 2008	PM_{10}		1.5	0.2		0.7	0.3	0.2	(Decesari et al., 2010)
			PM_1								
Mt. Fuji, Japan	3776	Jun2001-Aug 2002	TSP					1.2	0.1	0.3	(Suzuki et al., 2008)
Mt. Abu, India	1680	Annual 2008	TSP		3.7	0.5	1.2	2.9	0.6	0.4	(Rastogi and Sarin, 2005;Ram et al., 2008)
		Mar 2007-Feb 2008	$PM_{2.5}$					3.9	0.3	1.2	(Kumar and Sarin, 2010)
		Mar 2007-Feb 2008	$PM_{2.5-10}$					0.5	1.1		
Mt. Darjeeling, India	2200	Jan-Dec 2005	PM_{10}					2.5	1.0	0.1	(Chatterjee et al., 2010)
		Jan-Dec 2005	$PM_{2.5}$					3.8	3.3	0.9	
Manora Peak, India	1950	Winter 2004	TSP		8.7	1.1	2.3	2.6	0.5		(Rengarajan et al., 2007)
Yosemite NP, USA	1603	Jun-Sep 2002	PILS method					1.0	0.3	0.4	(Lee et al., 2008)
San Gorgonio, USA	1705	Apr-2003						0.6	3.2	0.9	
		Jul-2003						1.3	1.3	1.0	

1

3.2 Relatively aged chemical components with summer maximum found at the elevated site

Figure 2 summarized the average mass size distributions (MSDs) of organics, sulfate, nitrate and ammonium on annual and seasonal basis. The MSDs of these four chemical species in particles with diameters between 30 and 1000 nm were found to be approximately lognormal. The annually mass median diameters (MMDs) for bulk organics, sulfate, nitrate, and ammonium in entire observational period were quite similar with 538, 585, 540 and 541 nm, respectively. The standard deviations (σ_g) of the fitted MSDs were generally smaller than 2, showing that accumulation mode particles significantly impact the MSDs for each chemical component.

Seasonally, maximum MMDs for almost all chemical components were found in summer and fall, minimum in spring. During summer-half year, high temperature, high relative humidity and strong radiation enhanced oxidation reactions, under the stagnant meteorological condition, the aerosol will stay longer at the atmosphere, and the aged pollutants are prone to be transported to the site via the vertical convection process, which results in more aged aerosols. In the winter time, organics and nitrate display smaller MMDs than sulfate, indicating the organics and nitrate are fresher than sulfate. The local emissions from coal combustion and traffic are the main sources contributing to organics and nitrate, and the aged sulfate is from the regional transport. In addition, the smallest MMDs were found in springtime, which was due to the transport of relatively fresh aerosols from the north. Consequently, the relative larger MMDs were also found at this high elevated site than those at several ground sites in the NCP, including the sub-urban Gucheng station and sub-urban Tianjin (Zhang, 2011), and urban Beijing (Zhang et al., 2012d), showing the relative aged and regionally-dispersed fine aerosols received compared with those from ground-based measurement.

3.3 PBL, LFT, NPF events, in-cloud and polluted episodes

3.3.1 Mass concentration of chemical components for different episodes

In order to further explore the controlling factors on aerosols at this site, episodes influenced by planet boundary layer (PBL), lower free troposphere (LFT), new particle formation events (NPF), enveloped by cloud (in-cloud) and polluted episodes were classified following methods mentioned in section 2.3 throughout the entire campaign. Overall, the site was influenced by PBL and LFT at same frequency in spring and winter, while the site was influenced more by PBL than LFT in summer and fall. Cloud and polluted episodes occurred more frequently in summer and fall, and NPF events were observed mostly in spring.

Figure 3 shows the average mass concentration of PM_1 during these episodes. It is shown that the highest with 66 μg m^{-3} was from the polluted episode, and lowest was during NPF events from large contribution of ultrafine particles. The mass loading during PBL influence was slight higher than that during LFT (42 μg m^{-3}) and in cloud (40μg m^{-3}). This LFT mass level is about 2-10 times higher than that monitored during night time at Mount. JFJ (Cozic et al., 2008), NCO-P (Decesari et al., 2010) and Murodo (Kido et al., 2001). The relative high concentration at the free troposphere of Mt. Tai indicated that although the boundary layer decented lower than the site, almost 80% pollutants transported by the vertical convections stayed at low free troposphere or residual layer, and the pollutants from ground have impacted the air quality of the mountain site seriously.

The proportions of organics, sulfate, nitrate, ammonium and chloride in different episodes for PM_1 are presented in Figure 3 by pie charts, which show that organics and sulfate contribute distinct between in-cloud and NPF events. During the new particle formation events, the percentage of organics and sulfate was 37% and 22% respectively. Conversely, sulfate dominated the aerosols with 38% and organics contributed less with 24% in cloud episodes. The higher measured sulfate mass concentrations in the cloud residuals were also observed at the top of East Peak mountain in Cape San Juan (Allan et al., 2008). Most sulfate aerosols in the atmosphere are secondary sulfate

formed by the oxidation of gaseous precursors (SO_2), followed by particle formation through nucleation and condensation processes. There are several pathways for sulfate formation such as liquid-phase reactions inside cloud droplets or oxidation of SO_2 with OH via gaseous phase reactions (Calvo et al., 2012). As the saturation vapour of sulphuric acid is very low, it is not found in the gaseous phase in the troposphere but rather condenses rapidly to form droplets of a sulfuric acid solution. Under normal atmospheric conditions, these particles are partially or totally neutralised by ammonia (NH_3) and in the process, depending on relative humidity, they may become solids (Wang et al., 2008). In this case, ammonium sulfate is more stable in the atmosphere. Once there is sufficient water vapour supplying, it is possible that some of the mass could have been added in the cloud through aqueous processes, the sulfate-dominant particles were easier to be activated as CCN. Under the polluted background and limitation of water vapour, still some interstitial aerosol remained in the cloud and was measured by the AMS. The higher contribution of organics in NPF events indicates its significant role for the particle formation and growth process. The importance of organics in the atmospheric new particle formation was emphasized in several researches (Kulmala et al., 2013). Similar phenomenon was also observed and discussed in more details at ground site campaign in Beijing (Zhang et al., 2011). In terms of nitrate, ammonium and chloride, no dramatic variations on their proportions of PM_1 were observed in these episodes, meaning their minor roles at the different kind of episodes.

3.3.2 Mass size distributions of chemical components during different episodes

The MSDs of PM_1 (ΣOSNA), chemical species and their proportions at different size ranges during PBL, LFT, NPF events, in cloud and polluted episodes are plotted in Figure 4 and Figure 5. Totally, the MSDs of PM_1 for these episodes displayed accumulation mode with 600-700nm MMD, except smaller MMD (550nm) with wider size distribution for NPF. The standard deviation of the fitted MSD for NPF (σ=2.1) was larger than other episodes (σ=1.7-1.8) for the impact of small particles. Same MSDs for other events were found, indicating they may originate from similar sources or evolution process again.

Since NPF events being the significant sources of the aerosols, the links between MSDs of NPF events and polluted episodes can be employed to investigate the evolution of particles. Statistically results from all the NPF events and polluted episodes showed the comparatively small MMDs (~373–459 nm) for organics during NPF events at Mt. Tai and the larger MMDs (~473–792 nm) during polluted episodes. The nitrate and ammonium also displayed relative small MMDs during NPF than during polluted episodes. No obvious differences of sulfate MMDs between NPF events and polluted episodes were found, meaning sulfate was more aged than organics, nitrate and ammonium in NPF events. This phenomenon suggests sulfate may originate from regional polluted area, while organics, nitrate and ammonium from local sources. In this paper, the ratio in the value of MMD between the polluted episodes and NPF event was defined as increasing factor. The organics increasing factors in MMDs between NPF events and polluted episodes are larger than that of an urban ground site in Beijing (~38-61%), a suburban site in Wuqing (~27-32%), and a rural site in Gucheng (8-42%). The increasing factors for sulfate, nitrate and ammonium in Beijing were all lower than that at Mt. Tai. The increasing factors of MMD from NPF events to polluted episodes at Mt. Tai are smaller than those in less polluted areas. At a regional site in Pittsburgh, USA, the increasing factors for organics, sulfate, nitrate and ammonium from a nucleation event to polluted air were 165%, 200%, 29%, 160%, respectively. These data suggest the background level of aerosol would influence the evolution of MMDs, and the MMDs at a certain degree, i.e. the pollution level and particle aging.

As the MSDs of chemical species between PBL and LFT were very similar, the LFT's MSDs in Figure 5 was omitted. By investigating the MSDs and percentage of chemical species in different size mode, organics and sulfate were found to present different roles, while nitrate and ammonium displayed relative stable patterns. During PBL, NPF events and polluted episodes, organics accounted for major proportions at small mode, and organics was about 70% at 100-200 nm

particles in polluted episodes. Under episodes influenced by PBL and NPF, half of chemical species was organics for the particles around 100 nm, 20% from sulfate, another 20% from nitrate and 10% from ammonium. The larger the particle was, the more the sulfate contributed to the particles. In cloud episodes, sulfate contributed most fractions (60%) to the small particles (100-200nm), and dominated the particles through the whole size range of PM_1. Organics occupied less with 20% at small particles. The percentage of organics increased to maximum at 200-300nm, and fractions of nitrate and ammonium also increased accordingly. Totally, more than 70% of inorganics contributed to the PM_1 in cloud episodes. Due to the hygroscopicity of ammonium sulfate and ammonium nitrate, they were likely grown up by water uptake and partially participated in the cloud formation.

3.4 Transport pathways and associated chemical component changes

Seven main back-trajectory clusters were identified by using TrajStat and the HYSPLIT-4.8 model (Figure 6). Based on the distances of air masses transported, cluster 1, 2, and 3 were defined as short pathways, cluster 4 and 6 were mediums, and cluster 5 and 7 were considered as long transport pathway. Cluster-1 (~17% of the total) represents the shortest transport pathway, which was from the south. These trajectories passed over Xuzhou in Anhui Province, an area that suffers from serious pollution, mainly due to biomass burning (Wang et al., 2002;Woo et al., 2003;Suthawaree et al., 2010). Tai' an, a prefecture-level city, located on the southern flank of Mt. Tai, is a likely source for pollution when the airflow followed this pathway. Trajectories in Cluster-2 (~16%) started over the Yellow Sea and passed over the eastern side of the Shandong Peninsula. Air masses following this relatively short path would bring both marine aerosol and ground-level air pollutants to Mt. Tai. Cluster-3 (another ~ 25%) was from the north/northeast of Mt. Tai, starting at Chengde in Hebei Province and then passing through Bohai sea and Shandong Peninsula. The three short distance clusters account for ~60% of all the air masses, showing the majority of regionally-dispersed aerosol received at Mt. Tai was from short distance mixed aerosol, mostly from its south.

Cluster-4 (~7%) shows the airflow from north of China to the NCP, including Tianjin and Hebei Province. These trajectories are representative of regional-scale transport path. Trajectories in Cluster-5 (20%) originate over remote areas in north/north-west China with a transport path above 3000 m. These air masses swept through Hebei province to the site at high wind speed, which has assumed delivering most of aerosol in FT. Cluster-6 (~11%) represents regional transport from the west of Mt. Tai. Cluster-7 (4%) represents group of trajectories from the further northwest with longer distances. The air masses in these four clusters account for another ~40% of all transport, and bring less polluted aerosol from north. These can also be supported by the sums of the mass concentrations of the OSNAC of 51, 59 and 48 μg m^{-3} for the first three clusters aerosols, and 36, 16, 34 and 14 μg m^{-3} for the rest clusters respectively. The mass loadings for Cluster 5 and 7 were the lowest of seven clusters. Even though they are still much higher than those at Whistler Mt. (1.2 μg m^{-3}), they are close to a similar level to what has been observed at Korea and Japan (11–13 μg m^{-3}) (Zhang et al., 2007). The MMDs, standard deviations and mass concentrations of chemical components corresponding to the seven clusters are summarized in Table 2. Only mass concentrations but no size information for chloride is presented because no mass fragmentation of chloride was selected in time-of-flight (TOF) mode during the campaign. The relative smaller MMDs were also found for chemical components associated with long-distance transported aerosols (cluster 4-7), suggesting the relative fresh aerosols. While the larger MMDs for short clusters indicated that the aerosols were more aged.

Organics and sulfate were the two largest fractions, accounting for ~30% each for the ΣOSNAC in the airflow associated with the first three short-distant paths (cluster 1, 2 and 3) from the south (Table 2), demonstrating again the more pollutants from Pan-Yangtze river delta area. The nitrate was about 20% with mean concentrations of 9.0, 11.2, 10.9 μg m^{-3} for cluster 1, 2 and 3 respectively. The ammonium and chloride were the two smallest fractions with ~17% and 2%,

respectively. The much higher organics were found for aerosol travelled long-distance from north relative to the short-distance moving aerosols from south. About 40% organic were found in aerosols associated with cluster 4, 5, 6 and 7.

Table2. Mass median diameters (MMD, nm, standard deviations (σ_g) and mass concentration (Mass, μg m^{-3}) for chemical components in samples grouped by air-mass trajectory cluster

Air mass	Organics			Sulfate			Nitrate			Ammonium			Chloride
	MMD	σ_g	Mass	MMD	σ_g	Mass	MMD	σ_g	Mass	MMD	σ_g	mass	Mass
Cluster-1	545	1.7	16.8	570	1.7	15.6	582	1.7	9.0	542	1.7	8.7	0.9
Cluster-2	533	1.6	18.2	584	1.7	17.6	581	1.6	11.2	553	1.7	10.2	1.0
Cluster-3	511	1.7	16.4	528	1.8	11.4	514	1.7	10.9	497	1.8	8.1	1.2
Cluster-4	464	1.7	12.8	517	1.7	9.1	470	1.7	7.4	478	1.7	5.8	0.8
Cluster-5	458	1.6	6.8	515	2.0	3.7	462	2.1	2.9	440	2.0	2.5	0.5
Cluster-6	417	1.8	12.7	464	2.0	6.8	435	1.8	8.0	437	1.9	5.4	1.0
Cluster-7	426	2.0	5.2	459	1.9	3.4	357	2.3	2.5	395	2.2	2.1	0.4

3.5 **Composition of OA**

To further investigate the secondary OA, AMS-PMF modelling of OA spectra (Aiken et al., 2009;Ulbrich et al., 2009) was used to identify presumptive sources for the organic aerosol during each of four seasons at Mt Tai. Different types of organics were resolved based on specific mass-spectral profiles, and the mass concentrations are presented in Table 3. The mass spectra for Hydrocarbon-like OA (HOA) is characterized by hydrocarbon ions of the general form C_nH_{2n+1} and C_nH_{2n-1}, including $C_3H_7^+$ (m/z 43), $C_4H_7^+$ (m/z 55), and $C_4H_9^+$ (m/z 57). A signal from m/z 60, a tracer ion for biomass burning organic aerosol (BBOA) (Alfarra et al., 2006;Aiken et al., 2009), which can be attributable to POA (Jimenez et al., 2009), was resolved in the mass spectra from spring, summer and fall. In winter, another factor with high m/z 43 and m/z 60 was identified as the coal-combustion organic aerosol (CCOA) (Sun et al., 2013). The mass concentration of subtype organics and their percentage in organic matter are presented in Table 3. HOA, BBOA and CCOA can be considered as primary organic matter (POA) directly emitted into the atmosphere. The POA dominated OA during wintertime with 59% of organics, and accounting for 51%, 44% and 48% of OA in spring, summer, fall and winter, respectively. Same result was reported at a ground site in urban site Beijing in winter (Sun et al., 2013). BBOA was derived from AMS database by PMF model in spring, summer and fall. June every year in China is the high season for harvest of wheat, and also the period when straw burning takes place seriously in some part of the country (Qu et al., 2012). Previous study mentioned that field burning of wheat straws in the North China Plain during May–June 2006 in urban areas such as Beijing (Li et al., 2007). Study based on organic molecular compositions of Mt. Tai also identified levoglucosan in summer (Fu et al., 2008). It is deemed that agriculture residues burning, crop residues burning are the main sources of BBOA influenced the site. On the other hand, as a tourist spot, burning incense is a feature of Mt. Tai. Although some special incense burning events including weekends, holidays, and traditional festivals have been deleted in the datasets, incense burning probably is another BBOA source influence Mt. Tai on normal days, which needs further investigations. Assuming the emission of incense burning was constant, more BBOA was measured in summer than spring and fall, which suggests intensive emission from field burning of agriculture residues in summer. In winter, 37% of organics was identified as HOA and 22% as CCOA. Coal combustion in China has been found to emit a large quantity of carbonaceous aerosols, contributing 70% of total emitted PM2.5 (Zhang et al., 2012a). It is widely accepted that HOA is mainly associated with combustion-related emissions, e.g., diesel exhaust (Sun et al., 2013). The relatively high concentration of HOA in winter should result from the low ambient temperature, low atmospheric oxidants, and most of fresh traffic exhaust was

transported to the site with less oxidizations.

At Mt. Tai, one can still find other large fraction of oxygenated organic aerosol (OOA) that is considered to be secondary generally (Herndon et al., 2008;Volkamer et al., 2006), in which two subtypes of OOA can be distinguished by large fraction of CO_2^+ (m/z 44) for low-volatility oxidized organic aerosol (LV-OOA) and by $C_3H_7^+$ (m/z 43), CO_2^+ (m/z 44), $C_3H_3O^+$ (m/z 55) and $C_3H_5O^+$ (m/z 57) for semi-volatile oxidized organic aerosol (SV-OOA). LV-OOA is strongly correlated with non-volatile secondary species such as sulfate and has a high O:C, mainly attributable to regional, heavily aged OA; SV-OOA has a higher correlation with semi-volatile species such as ammonium nitrate and ammonium chloride and has a lower O:C, consistent with less–photo chemically fresh OA (Jimenez et al., 2009). SV-OOA and LV-OOA together contributed 49%, 55%, 51% and 41% from spring to winter. More OOA was observed in summer which attributed to the strong photochemical reaction, sufficient oxidization process along with regional disperse in the CEC. This identification about relative contributions of POA and SOA is similar to a 2-yr filter measurement from 16 sites in various regions of China, which reported that the secondary organic carbon contributed ~55% and 60% for urban and rural aerosol, respectively(Zhang et al., 2012c).

Table3. Seasonal averaged mass concentrations (unit: μg m^{-3}) and standard deviation with percentage (in parentheses) of specific types of organic aerosols from Positive matrix factorization analysis

Sub-type organics [a]	Spring	Summer	Fall	Winter
Primary OA				
HOA	2.3±1.2 (27%)	1.6±1.8 (10%)	0.60±0.38 (11%)	5.6±1.6 (37%)
BBOA	2.1±1.1 (24%)	5.1±10.7 (34%)	1.1±0.65 (19%)	
CCOA			1.1±0.61 (19%)	3.3±2.2 (22%)
Secondary OA				
SV-OOA		3.1±4.2 (21%)		
LV-OOA	4.2±2.3 (49%)	5.3±6.4 (35%)	2.9±1.59 (51%)	6.1±3.56 (41%)

[a]Abbreviations: HOA = hydrocarbon-like organic aerosol, BBOA = biomass-burning organic aerosol, CCOA= coal combustion organic aerosol, semi-volatile oxidized organic aerosol = SV-OOA, and low-volatility oxidized organic aerosol = LV-OOA.

4 Summary

The mass concentrations and size distributions of chemical components in PM_1 were characterized in situ with an AMS at the summit of Mt. Tai (~1500 m a.s.l) from June 2010 to January 2012.

The mass concentration of organics, sulfate, nitrate, ammonium and chloride (OSNAC) in PM_1 at Mt. Tai is higher than those at most mountain sites in the USA and Europe, but comparable with previous research results at Mt. Tai. Seasonally, high concentrations of all chemical components in ~1500 m high level were found in summer with minimum in fall, slightly different from typical seasonal patterns in various aerosol components at ground-based measurement in China ("spring minimum"). This seasonal pattern was controlled by the development of PBL, horizontal transportation and local emissions.

The MSDs for organics, sulfate, nitrate and ammonium were approximately log-normal with more than 99% mass fraction attributable to the particle with diameter larger than 100 nm. Different from the seasonality of mass concentrations, maximum MMDs for almost all chemical components were found in summer and secondary high values in fall with minimum in spring, indicating the summer-half of the year was more conducive for the formation of aged fine aerosols. The larger MMDs are found at Mt. Tai than those in ground sites, showing the relative aged and well-mixed

aerosol observed. The smaller MMDs were found for organics of the NPF events compared to the aged episodes with MMDs of ~473–792 nm. Compared with MMD of organics between NPF events and polluted episodes at Mt. Tai, small increasing factors have been reported at an urban ground site in Beijing (~38-61%), a suburban site in Wuqing (~27-32%), and a rural site in Gucheng (8-42%). Larger increasing factors for sulfate, nitrate and ammonium were found in less polluted site in Europe and USA. The MMDs of chemical species could indicate the polluted level and particle aging to a certain degree.

Five kinds of episodes influenced by PBL, LFT, NPF events, in-cloud and polluted episodes at Mt. Tai were classified. The highest mass concentration was observed during polluted episodes with large MMD and lowest in NPF events with relatively small MMD. The LFT was 80% of PBL, indicating most of pollutants in PBL could be transported to the low free troposphere. For chemical species, organics dominated the PBL, NPF events and polluted episodes and sulfate dominated in cloud episodes. There were no obvious variations on proportions of nitrate and ammonium in five kinds of episodes. In cloud, inorganics contributed 70% to the PM_1 at the whole size range, and sulfate dominated with 40% to the small mode particles, while organics was 20% of small mode particles. The larger quantities of inorganics in particles make it easier to add into the cloud through water uptake.

The air-mass back trajectories were grouped into seven clusters. Three of the clusters regional exemplified transport from the north, east, and south of Mt. Tai; two medium length clusters were from the northwest and west of site, and two long-range clusters showed airflow from the northwest of the site. Shorter transport pathways were corresponded with higher aerosol mass concentrations. The analysis of transport showed that the air quality at Mt. Tai was impacted by the pollution from the Shandong Peninsula, the NCP and areas immediately north of Suzhou. The air masses represented by clusters 5 and 7 brought the clean, dry air from the northwest, which swept pollution away from the site.

At Mt. Tai, one can still find the large fraction (normally half) of total OA can be attributable to oxygenated organic aerosol (OOA) that is considered to be secondary generally. Extra high proportions of SOA found in summer, presenting the intensive solar radiation and oxidized process. Regionally, heavily aged OA were observed with >40% OOA. Hydrocarbon-like OA (HOA), biomass burning organic aerosol (BBOA) and coal-combustion organic aerosol (CCOA) were considered as primary organic matter (POA) directly emitted into the atmosphere, and accounted together for 51%, 44%, 48% and 59% of the total measured organics in spring, summer, fall and winter, respectively. Considerable amount of BBOA in summer and CCOA in winter were found with 34% and 22% of OA respectively.

Acknowledgements. This research was supported by National Key Project of Basic Research (2011CB403401, 2014CB441303), National Nature Science Foundation of China (41275141; 41175113) and Specific Team Fund from NJU Collaborative Innovation Center on climate change.

References

Aiken, A. C., Salcedo, D., Cubison, M. J., Huffman, J. A., DeCarlo, P. F., Ulbrich, I. M., Docherty, K. S., Sueper, D., Kimmel, J. R., and Worsnop, D. R.: Mexico City aerosol analysis during MILAGRO using high resolution aerosol mass spectrometry at the urban supersite (T0)-Part 1: Fine particle composition and organic source apportionment, Atmos. Chem. Phys., 9, 6633-6653, 2009.

Albrecht, B. A.: Aerosols, cloud microphysics, and fractional cloudiness, Science, 245, 1227-1230, 1989.

Alfarra, M. R., Paulsen, D., Gysel, M., Garforth, A. A., Dommen, J., Prévôt, A. S. H., Worsnop, D. R., Baltensperger, U., and Coe, H.: A mass spectrometric study of secondary organic aerosols formed from the photooxidation of anthropogenic and biogenic precursors in a reaction chamber, Atmos. Chem. Phys., 6, 5279-5293, 2006.

Allan, J. D., Baumgardner, D., Raga, G. B., Mayol-Bracero, O. L., Morales-García, F., García-García, F., Montero-Martinez, G., Borrmann, S., Schneider, J., and Mertes, S.: Clouds and aerosols in Puerto Rico-a new evaluation, Atmos. Chem. Phys., 8, 1293-1309, 2008.

Boucher, O., Randall, D., Artaxo, P., Bretherton, C., Feingold, G., Forster, P., Kerminen, V.-M., Kondo, Y., Liao, H., Lohmann, U., Rasch, P., Satheesh, S. K., Sherwood, S., Stevens, B., and Zhang, X. Y.: Clouds and Aerosols, in: Climate Change 2013: The Physical Science Basis. Contribution of Working Group I to the Fifth Assessment Report of the Intergovernmental Panel on Climate Change, edited by: Stocker, T. F., D. Qin, G.-K. Plattner, M. Tignor, S. K. Allen, J. Boschung, A. Nauels, Y. Xia, V. Bex and P. M. Midgley, Cambridge University Press, New York, 2013.

Calvo, A. I., Alves, C., Castro, A., Pont, V., Vicente, A. M., and Fraile, R.: Research on aerosol sources and chemical composition: Past, current and emerging issues, Atmos. Res., 120-121, 1-28, 2012.

Charlson, R. J., Schwartz, S. E., Hales, J. M., Cess, R. D., Coakley, j. J. A., Hansen, J. E., and Hofmann, D. J.: Climate forcing by anthropogenic aerosols, Science, 255, 423-430, 1992.

Chatterjee, A., Adak, A., Singh, A. K., Srivastava, M. K., Ghosh, S. K., Tiwari, S., Devara, P. C., and Raha, S.: Aerosol chemistry over a high altitude station at northeastern Himalayas, India, PloS one, 5, e11122, 2010.

Cozic, J., Verheggen, B., Weingartner, E., Crosier, J., Bower, K., Flynn, M., Coe, H., Henning, S., Steinbacher, M., and Henne, S.: Chemical composition of free tropospheric aerosol for PM1 and coarse mode at the high alpine site Jungfraujoch, Atmos. Chem. Phys., 8, 407-423, 2008.

Decesari, S., Facchini, M. C., Fuzzi, S., McFiggans, G. B., Coe, H., and Bower, K. N.: The water-soluble organic component of size-segregated aerosol, cloud water and wet depositions from Jeju Island during ACE-Asia, Atmos. Environ., 39, 211-222, 2005.

Decesari, S., Facchini, M., Carbone, C., Giulianelli, L., Rinaldi, M., Finessi, E., Fuzzi, S., Marinoni, A., Cristofanelli, P., and Duchi, R.: Chemical composition of PM 10 and PM 1 at the high-altitude Himalayan station Nepal Climate Observatory-Pyramid (NCO-P)(5079 m asl), Atmos. Chem. Phys., 10, 4583-4596, 2010.

Fu, P., Kawamura, K., Okuzawa, K., Aggarwal, S. G., Wang, G., Kanaya, Y., and Wang, Z.: Organic molecular compositions and temporal variations of summertime mountain aerosols over Mt. Tai, North China Plain, J. Geophys. Res., 113, D19107, doi:10.1029/2008JD009900, 2008.

Fu, P., Kawamura, K., Kanaya, Y., and Wang, Z.: Contributions of biogenic volatile organic compounds to the formation of secondary organic aerosols over Mt. Tai, Central East China, Atmos. Environ., 44, 4817-4826, 2010.

Gallagher, J. P., McKendry, I. G., Macdonald, A. M., and Leaitch, W. R.: Seasonal and diurnal variations in aerosol concentration on Whistler Mountain: Boundary layer influence and synoptic-scale controls, J. Appl. Meteorol., 50, 2210-2222, 2011.

Henning, S., Weingartner, E., Schwikowski, M., Gäggeler, H., Gehrig, R., Hinz, K. P., Trimborn, A., Spengler, B., and Baltensperger, U.: Seasonal variation of water‐soluble ions of the aerosol at the high‐alpine site Jungfraujoch (3580 m asl), J. Geophys. Res., 108, 4030, doi:4010.1029/2002JD002439, 2003.

Herndon, S. C., Onasch, T. B., Wood, E. C., Kroll, J. H., Canagaratna, M. R., Jayne, J. T., ..., and Worsnop, D. R.: Correlation of secondary organic aerosol with odd oxygen in Mexico City, Geophys. Res. Lett., 35, L15804, 2008.

Jayne, J. T., Leard, D. C., Zhang, X., Davidovits, P., Smith, K. A., Kolb, C. E., and Worsnop, D. R.: Development of an aerosol mass spectrometer for size and composition analysis of submicron particles, Aerosol.Sci.TechnoL., 33, 49-70, 2000.

Jimenez, J. L., Canagaratna, M. R., Donahue, N. M., and Worsnop, D. R.: Evolution of Organic Aerosols in the Atmosphere, Science, 326, 1525, DOI: 10.1126/science.1180353, 2009.

Kido, M., Osada, K., Matsunaga, K., and Iwasaka, Y.: Diurnal variation of ionic aerosol species and water‐soluble gas concentrations at a high‐elevation site in the Japanese Alps, J. Geophys. Res., 106, 17335-17345, 2001.

Kulmala, M., Vehkamäki, H., Petäjä, T., Dal Maso, M., Lauri, A., Kerminen, V. M., Birmili, W., and McMurry, P. H.: Formation and growth rates of ultrafine atmospheric particles: a review of observations, J. Aerosol. Sci., 35, 143-176, 2004.

Kulmala, M., Kontkanen, J., Junninen, H., Lehtipalo, K., Manninen, H. E., Nieminen, T., Petäjä, T., Sipilä, M., Schobesberger, S., and Rantala, P.: Direct observations of atmospheric aerosol nucleation, Science, 339, 943-946, 2013.

Kumar, A., and Sarin, M.: Atmospheric water-soluble constituents in fine and coarse mode aerosols from high-altitude site in western India: Long-range transport and seasonal variability, Atmos. Environ., 44, 1245-1254, 2010.

Lanz, V. A., Alfarra, M. R., Baltensperger, U., Buchmann, B., Hueglin, C., and Prévôt, A. S. H.: Source apportionment of submicron organic aerosols at an urban site by factor analytical modelling of aerosol mass spectra, Atmos. Chem. Phys., 7, 1503-1522, 2007.

Lee, T., Yu, X. Y., Kreidenweis, S. M., Malm, W. C., and Collett, J. L.: Semi-continuous measurement of PM2.5 ionic composition at several rural locations in the United States, Atmos. Environ., 42, 6655-6669, 2008.

Li, W. J., Zhang, D. Z., Shao, L. Y., Zhou, S. Z., and Wang, W. X.: Individual particle analysis of aerosols collected under haze and non-haze conditions at a high-elevation mountain site in the North China plain, Atmos. Chem. Phys., 11, 11733-11744, 2011.

Li, X., Wang, S., Duan, L., Hao, J., Li, C., Chen, Y., and Yang, L.: Particulate and trace gas emissions from open burning of wheat straw and corn stover in China, Environ. Sci. TechnoL., 41, 6052-6058, 2007.

Qu, C., Li, B., Wu, H., and Giesy, J. P.: Controlling air pollution from straw burning in China calls for efficient recycling, Environ. Sci. TechnoL., 46, 7934-7936, 2012.

Ram, K., Sarin, M., and Hegde, P.: Atmospheric abundances of primary and secondary carbonaceous species at two high-altitude sites in India: Sources and temporal variability, Atmos. Environ., 42, 6785-6796, 2008.

Ramgolam, K., Favez, O., Cachier, H., Gaudichet, A., Marano, F., Martinon, L., and Baeza-Squiban, A.: Size-partitioning of an urban aerosol to identify particle determinants involved in the proinflammatory response induced in airway epithelial cells, Part. Fibre. Toxicol., 6, 1-12, 2009.

Rastogi, N., and Sarin, M.: Long-term characterization of ionic species in aerosols from urban and high-altitude sites in western India: Role of mineral dust and anthropogenic sources, Atmos. Environ., 39, 5541-5554, 2005.

Ren, Y., Ding, A., Wang, T., Shen, X., Guo, J., Zhang, J., Wang, Y., Xu, P., Wang, X., and Gao, J.: Measurement of gas-phase total peroxides at the summit of Mount Tai in China, Atmos. Environ., 43, 1702-1711, 2009.
Rengarajan, R., Sarin, M., and Sudheer, A.: Carbonaceous and inorganic species in atmospheric aerosols during wintertime over urban and high‐altitude sites in North India, J. Geophys. Res., 112, D21307, doi:21310.21029/22006JD008150, 2007.
Seinfeld, J. H., Carmichael, G. R., Arimoto, R., Conant, W. C., Brechtel, F. J., Bates, T. S., Cahill, T. A., Clarke, A. D., Doherty, S. J., and Flatau, P. J.: ACE-ASIA-Regional climatic and atmospheric chemical effects of Asian dust and pollution, B. Am. Meteorol. Soc., 85, 367-380, 2004.
Solomon, S., Qin, D., Manning, M., Chen, Z., Marquis, M., Averyt, K. B., Tignor, M., and Miller, H. L.: The physical science basis, Contribution of working group I to the fourth assessment report of the intergovernmental panel on climate change, 235-337, 2007.
Sun, J. Y., Zhang, Q., Canagaratna, M. R., Zhang, Y. M., Ng, N. L., Sun, Y. L., Jayne, J. T., Zhang, X. C., Zhang, X. Y., and Worsnop, D. R.: Highly time-and size-resolved characterization of submicron aerosol particles in Beijing using an Aerodyne Aerosol Mass Spectrometer, Atmos. Environ., 44, 131-140, 2010.
Sun, Y. L., Zhang, Q., Macdonald, A. M., Hayden, K., Li, S. M., Liggio, J., Liu, P. S. K., Anlauf, K. G., Leaitch, W. R., and Steffen, A.: Size-resolved aerosol chemistry on Whistler Mountain, Canada with a high-resolution aerosol mass spectrometer during INTEX-B, Atmos. Chem. Phys., 9, 3095-3111, 2009.
Sun, Y. L., Wang, Z. F., Fu, P. Q., Yang, T., Jiang, Q., Dong, H. B., Li, J., and Jia, J. J.: Aerosol composition, sources and processes during wintertime in Beijing, China, Atmos. Chem. Phys., 13, 4577-4592, 2013.
Suthawaree, J., Kato, S., Okuzawa, K., Kanaya, Y., Pochanart, P., Akimoto, H., Wang, Z., and Kajii, Y.: Measurements of volatile organic compounds in the middle of Central East China during Mount Tai Experiment 2006 (MTX2006): observation of regional background and impact of biomass burning, Atmos. Chem. Phys., 10, 1269-1285, 2010.
Suzuki, I., Hayashi, K., Igarashi, Y., Takahashi, H., Sawa, Y., Ogura, N., Akagi, T., and Dokiya, Y.: Seasonal variation of water-soluble ion species in the atmospheric aerosols at the summit of Mt. Fuji, Atmos. Environ., 42, 8027-8035, 2008.
Tuch, T. M., Haudek, A., Müller, T., Nowak, A., Wex, H., and Wiedensohler, A.: Design and performance of an automatic regenerating adsorption aerosol dryer for continuous operation at monitoring sites, Atmos. Meas. Tech., 2, 1143-1160, 2009.
Twomey, S.: Pollution and the planetary albedo, Atmos. Environ., 8, 1251-1256, 1974.
Ulbrich, I. M., Canagaratna, M. R., Zhang, Q., Worsnop, D. R., and Jimenez, J. L.: Interpretation of organic components from Positive Matrix Factorization of aerosol mass spectrometric data, Atmos. Chem. Phys., 9, 2891-2918, 2009.
Volkamer, R., Jimenez, J. L., San Martini, F., Dzepina, K., Zhang, Q., Salcedo, D., Molina, L. T., Worsnop, D. R., and Molina, M. J.: Secondary organic aerosol formation from anthropogenic air pollution: Rapid and higher than expected, Geophys. Res. Lett., 33, L17811, doi:10.1029/2006GL026899, 2006.
Wang, G., Li, J., Cheng, C., Hu, S., Xie, M., Gao, S., Zhou, B., Dai, W., Cao, J., and An, Z.: Observation of atmospheric aerosols at Mt. Hua and Mt. Tai in central and east China during spring 2009-Part 1: EC, OC and inorganic ions, Atmos. Chem. Phys, 11, 4221-4235, 2011.
Wang, J., Hoffmann, A. A., Park, R. J., Jacob, D. J., and Martin, S. T.: Global distribution of solid and aqueous sulfate aerosols: Effect of the hysteresis of particle phase transitions, J. Geophys. Res., 113, D11206, doi:11210.11029/12007JD009367, 2008.
Wang, T., Cheung, T. F., Li, Y. S., Yu, X. M., and Blake, D. R.: Emission characteristics of CO, NOx, SO2 and indications of biomass burning observed at a rural site in eastern China, J. Geophys. Res., 107, D12, 4157, 10.1029/2001JD000724, 2002.

Wang, Y. Q., Zhang, X. Y., and Draxler, R. R.: TrajStat: GIS-based software that uses various trajectory statistical analysis methods to identify potential sources from long-term air pollution measurement data, Environ. Model. Soft., 24, 938-939, 2009.
Watson, J.: Visibility: Science and Regulation, J. Air Waste Manage., 52, 628-713, 2002.
Woo, J., Streets, D. G., Carmichael, G. R., Tang, Y., Yoo, B., Lee, W., Thongboonchoo, N., Pinnock, S., Kurata, G., and Uno, I.: Contribution of biomass and biofuel emissions to trace gas distributions in Asia during the TRACE-P experiment, J. Geophys. Res., 108, 2156-2202, 2003.
Xiao, R., Takegawa, N., Zheng, M., Kondo, Y., Miyazaki, Y., Miyakawa, T., Hu, M., Shao, M., Zeng, L., and Gong, Y.: Characterization and source apportionment of submicron aerosol with aerosol mass spectrometer during the PRIDE-PRD 2006 campaign, Atmos. Chem. Phys., 11, 6911-6929, 2011.
Yamaji, K., Li, J., Uno, I., Kanaya, Y., Irie, H., Takigawa, M., Komazaki, Y., Pochanart, P., Liu, Y., and Tanimoto, H.: Impact of open crop residual burning on air quality over Central Eastern China during the Mount Tai Experiment 2006 (MTX2006), Atmos. Chem. Phys., 10, 7353-7368, 2010.
Yang, D., Yu, X., Fang, X., Wu, F., and Li, X.: A study of aerosol at regional background stations and baseline station, J. Appl. Meteorol., 7, 396–405, 1996
Zhang, H., Wang, S., Hao, J., Wan, L., Jiang, J., Zhang, M., Mestl, H. E. S., Alnes, L. W. H., Aunan, K., and Mellouki, A. W.: Chemical and size characterization of particles emitted from the burning of coal and wood in rural households in Guizhou, China, Atmos. Environ, 51, 94–99, 2012a.
Zhang, N., Cao, J., Ho, K., and He, Y.: Chemical characterization of aerosol collected at Mt. Yulong in wintertime on the southeastern Tibetan Plateau, Atmos. Res., 107, 76-85, 2012b.
Zhang, Q., Jimenez, J. L., Canagaratna, M. R., Allan, J. D., Coe, H., Ulbrich, I., Alfarra, M. R., Takami, A., Middlebrook, A. M., and Sun, Y. L.: Ubiquity and dominance of oxygenated species in organic aerosols in anthropogenically-influenced Northern Hemisphere midlatitudes, Geophys. Res. Lett., 34, L13801, 2007.
Zhang, X. Y., Wang, Y. Q., Zhang, X. C., Guo, W., Niu, T., Gong, S. L., Yin, Y., Zhao, P., Jin, J. L., and Yu, M.: Aerosol monitoring at multiple locations in China: contributions of EC and dust to aerosol light absorption, Tellus. B., 60, 647-656, 2008.
Zhang, X. Y., Wang, Y. Q., Niu, T., Zhang, X. C., Gong, S. L., Zhang, Y. M., and Sun, J. Y.: Atmospheric aerosol compositions in China: spatial/temporal variability, chemical signature, regional haze distribution and comparisons with global aerosols, Atmos. Chem. Phys., 12, 779-799, doi:10.5194/acp-12-779-2012, 2012c.
Zhang, Y. M.: Characterization of sub-micron aerosol and its change processes in BIV (Beijing and its vicinity) region, PhD, Chinese Academy of Meteorological Sciences, Beijing, 2011.
Zhang, Y. M., Zhang, X. Y., Sun, J. Y., Lin, W. L., Gong, S. L., Shen, X. J., and Yang, S.: Characterization of new particle and secondary aerosol formation during summertime in Beijing, China, Tellus. B., 63, 382-394, 2011.
Zhang, Y. M., Sun, J. Y., Zhang, X. Y., Shen, X. J., Wang, T. T., and Qin, M. K.: Seasonal characterization of components and size distributions for submicron aerosols in Beijing, Sci. China. Earth. Sci., 1-11, 2012d.
Zhou, C. H., Gong, S., Zhang, X. Y., Liu, H. L., Xue, M., Cao, G. L., An, X. Q., Che, H. Z., Zhang, Y. M., and Niu, T.: Towards the improvements of simulating the chemical and optical properties of Chinese aerosols using an online coupled model-CUACE/Aero, Tellus. B., 64, 1-20, 2012.
Zhou, Y., Wang, T., Gao, X., Xue, L., Wang, X., Wang, Z., Gao, J., Zhang, Q., and Wang, W.: Continuous observations of water-soluble ions in PM2. 5 at Mount Tai (1534 m asl) in central-eastern China, J. Atmos. Chem., 64, 107-127, DOI 10.1007/s10874-010-9172-z, 2009.

Figure Captions

Fig. 1. Correlation between AMS and (reconstructed) SMPS mass concentrations
Fig. 2. Mass size distributions of chemical species in annually and seasonally scale
Fig. 3. Mass concentrations of chemical components in different episodes
Fig. 4. The MSDs of PM_1 in different episodes
Fig. 5. The MSDs and proportions of chemical species in different episodes
Fig. 6. Averaged mass concentrations, mass-size distribution and percentage of chemical components associating with different air-mass trajectory clusters

Fig.1.

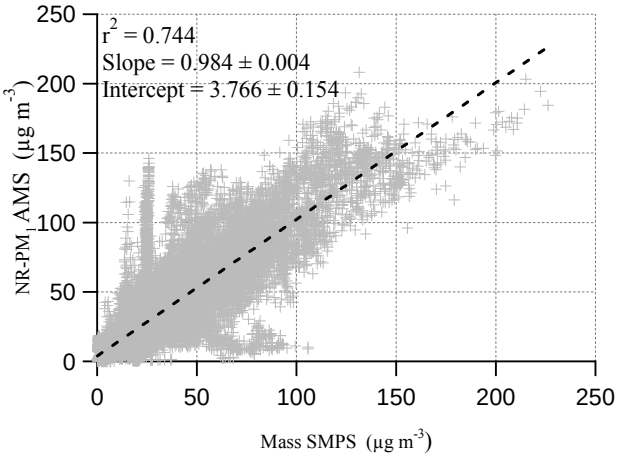
r² = 0.744
Slope = 0.984 ± 0.004
Intercept = 3.766 ± 0.154
NR-PM1 AMS (µg m-3)
Mass SMPS (µg m-3)
0
50
100
150
200
250

Fig.2.

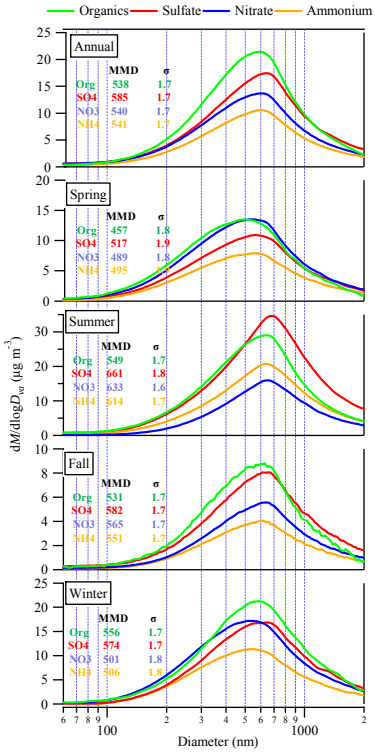
Organics
Sulfate
Nitrate
Ammonium
Annual
MMD σ
Org 538 1.7
SO4 585 1.7
NO3 540 1.7
NH4 541 1.7
Spring
MMD σ
Org 457 1.8
SO4 517 1.9
NO3 489 1.8
NH4 495
Summer
MMD σ
Org 549 1.7
SO4 661 1.8
NO3 533 1.6
NH4 514 1.7
Fall
MMD σ
Org 531 1.7
SO4 582 1.7
NO3 565 1.7
NH4 551 1.7
Winter
MMD σ
Org 556 1.7
SO4 574 1.7
NO3 501 1.8
NH4 506 1.8
dM/dlogD_va (μg m^-3)
Diameter (nm)
100
1000

Fig.3.

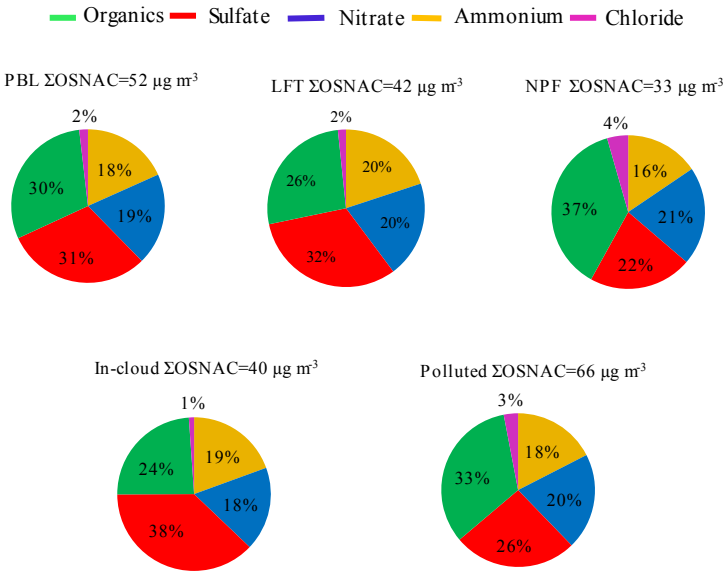
Organics
Sulfate
Nitrate
Ammonium
Chloride
PBL ΣOSNAC=52 μg m-3
2%
18%
19%
31%
30%
LFT ΣOSNAC=42 μg m-3
2%
20%
20%
32%
26%
NPF ΣOSNAC=33 μg m-3
4%
16%
21%
22%
37%
In-cloud ΣOSNAC=40 μg m-3
1%
19%
18%
38%
24%
Polluted ΣOSNAC=66 μg m-3
3%
18%
20%
26%
33%

Fig.4.

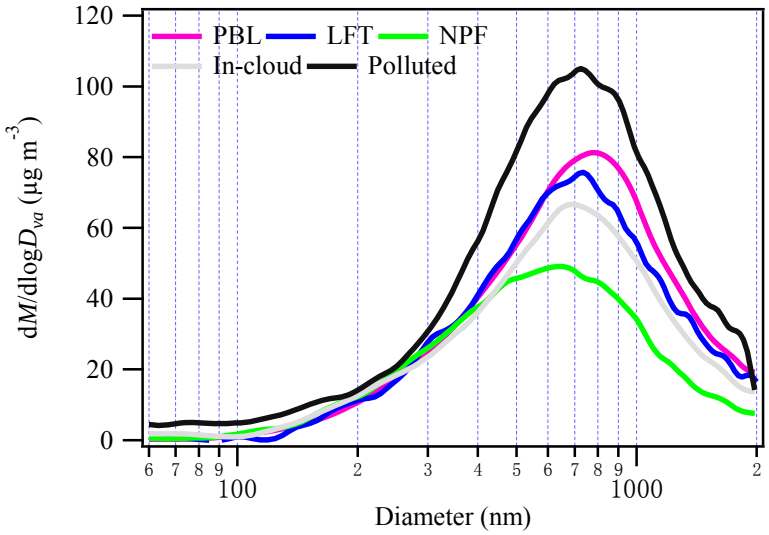
PBL
LFT
NPF
In-cloud
Polluted
dM/dlogDva (μg m-3)
120
100
80
60
40
20
0
6 7 8 9
100
2
3
4
5
6 7 8 9
1000
2
Diameter (nm)

Fig.5.

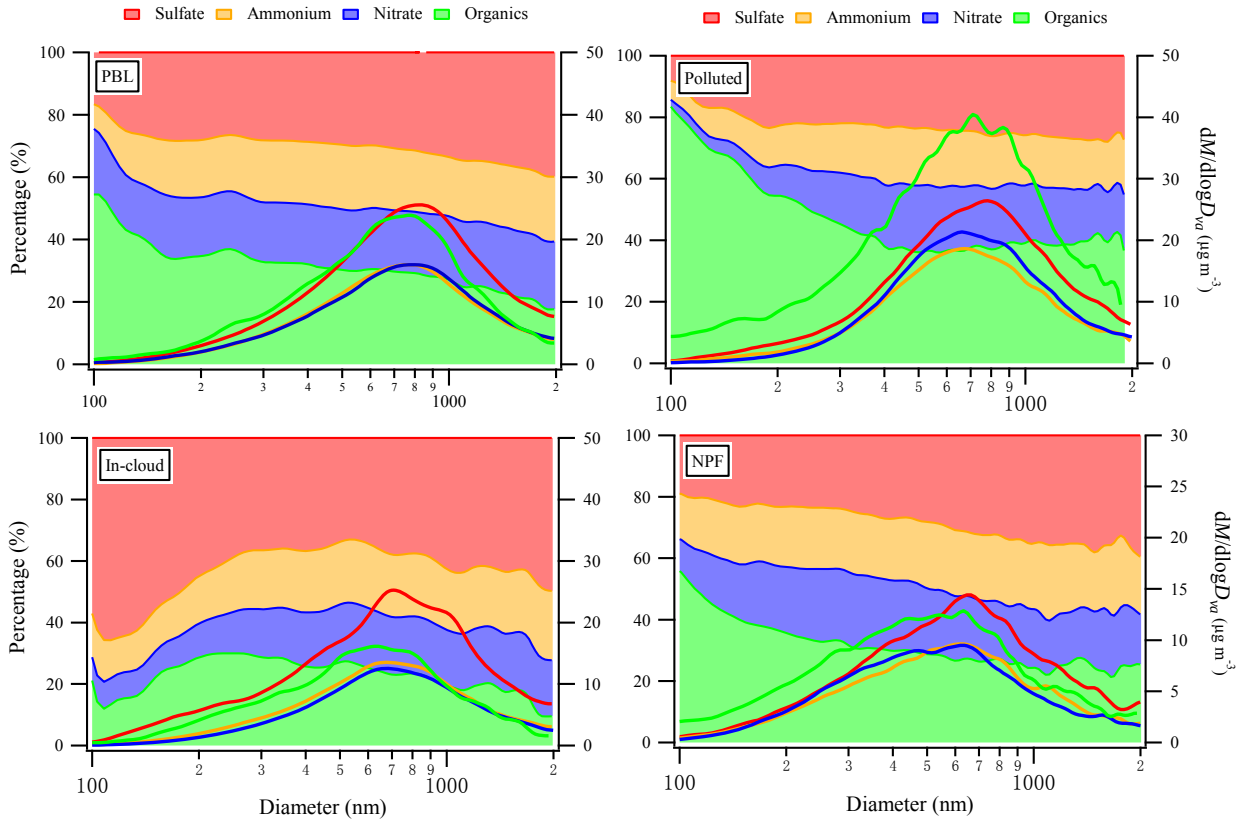
Sulfate
Ammonium
Nitrate
Organics
PBL
Polluted
In-cloud
NPF
Percentage (%)
dM/dlogDva (μg m-3)
Diameter (nm)

Fig. 6

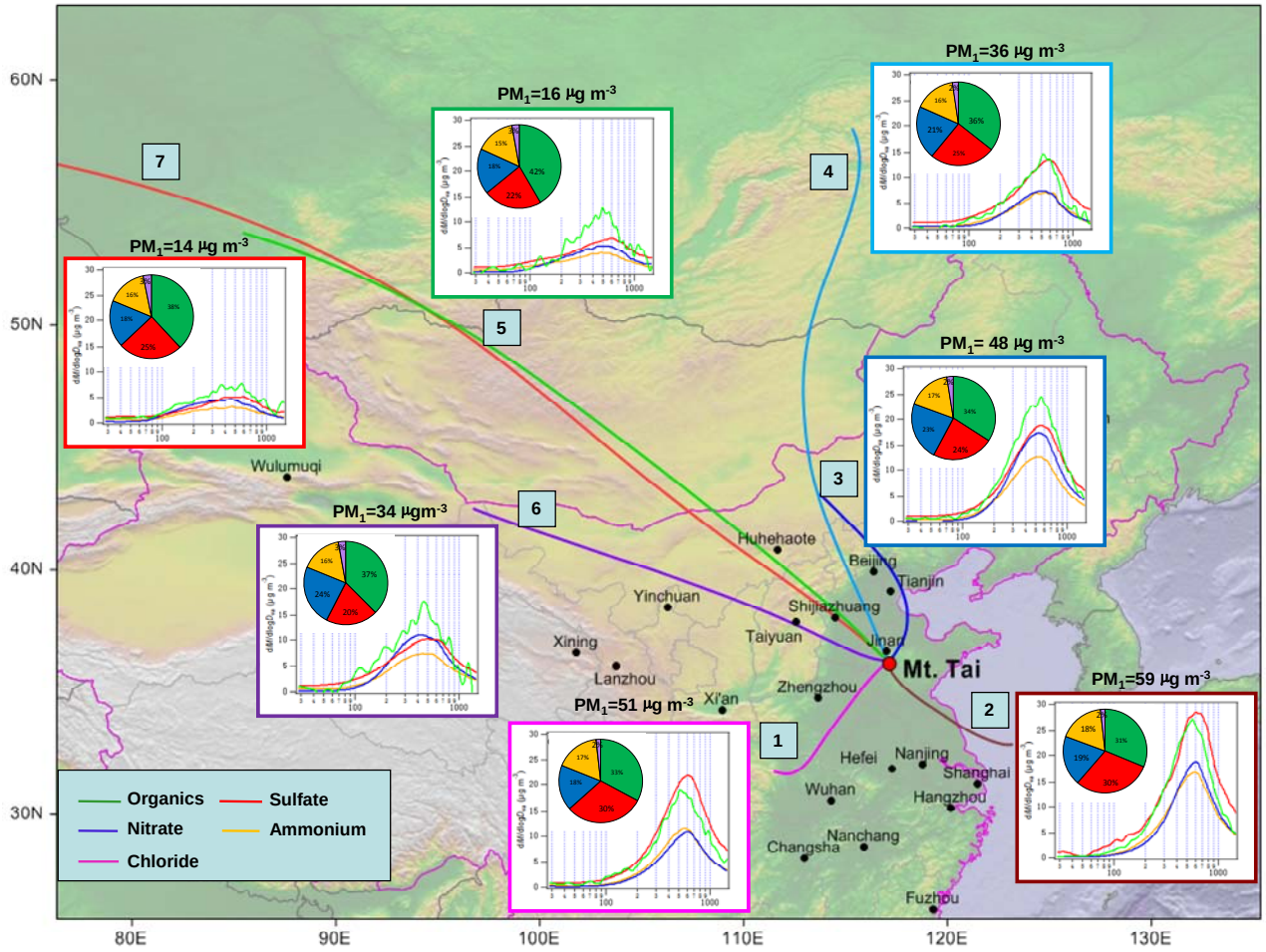
PM1=16 μg m-3
PM1=36 μg m-3
PM1=14 μg m-3
PM1= 48 μg m-3
PM1=34 μgm-3
PM1=51 μg m-3
PM1=59 μg m-3
7
4
5
3
6
1
2
Organics
Sulfate
Nitrate
Ammonium
Chloride
Wulumuqi
Huhehaote
Beijing
Tianjin
Yinchuan
Shijiazhuang
Taiyuan
Jinan
Xining
Lanzhou
Zhengzhou
Xi'an
Mt. Tai
Hefei
Nanjing
Shanghai
Wuhan
Hangzhou
Nanchang
Changsha
Fuzhou
60N
50N
40N
30N
80E
90E
100E
110E
120E
130E